Design and Realization of CPW Multilayer Couplers for Broadband Applications

V. T. Vo, L. Krishnamurthy, Q. Sun, G. Parkinson and A. A. Rezazadeh

The Electromagnetic Centre for Microwave and mm-Wave Designs and Applications,
School of Electrical and Electronic Engineering, The University of Manchester,
Sackville Street, PO Box 88, Manchester, UK, M60 1QD

Abstract

This paper describes the design and performance of wide band multi-octave passive MMIC couplers, which uses coplanar waveguide (CPW) multilayer techniques. The multilayer couplers are fabricated on GaAs semi-insulating substrate and are reciprocal and directional. On-wafer RF measurements were carried out on the fabricated multilayer directional couplers. Multilayer quadrature directional couplers with coupling factor and isolation better 5 dB and 20 dB are realized over 10 to 30 GHz. The relative merits of the performance and implementations of these passive couplers are compared to that of an active coupler based on GaAs pHEMT devices in view of their respective applications.

Keywords: Directional Couplers, MMICs, Multilayer Circuits

Introduction

Directional couplers are used in MMICs to realize balanced amplifiers, mixers and phase shifters. It is very important to select the correct technology, especially where the cost and circuit limitations are of prime importance. Active couplers can be designed and produced using a standard foundry process and can be made broadband by adapting the distributed amplifier circuit topology [1]. The distributed amplifier is inherently broadband and the modifications made to the circuit to produce a coupler increase the bandwidth and reduce the size of the circuit. However, active couplers have limitations where linearity and power are the prime parameters. Also they are not suitable for applications where a directional coupler would be used. An alternative to active couplers are passive couplers, which are reciprocal by their nature and can be used for many coupling applications provided the coupler's parameters can be maintained over a suitable bandwidth [2]. Conventional CPW couplers are normally realised by placing two transmission lines very close to each other, thus edge coupling mechanism was employed [3]. This design requires narrow gaps between the two transmission lines and coupling depends on the physical size of this gap. This construction inevitably incurred greater losses due to current crowding effect. To obtain tight coupling and low loss characteristics in this study a combination of both edge coupling and offset parallel broadside coupling has been designed employing the multilayer technique. Also compact spiral coupler is presented which uses a wound multilayer coupler in order to reduce the area occupied in MMIC chip.

In this paper, we present the design, fabrication and characterisation of some novel multilayer coupler structures. The results of microwave characterisation of the fabricated multilayer couplers are given and compared to that of an active coupler based GaAs pHEMT devices.

Design and Fabrications of Multilayer Couplers

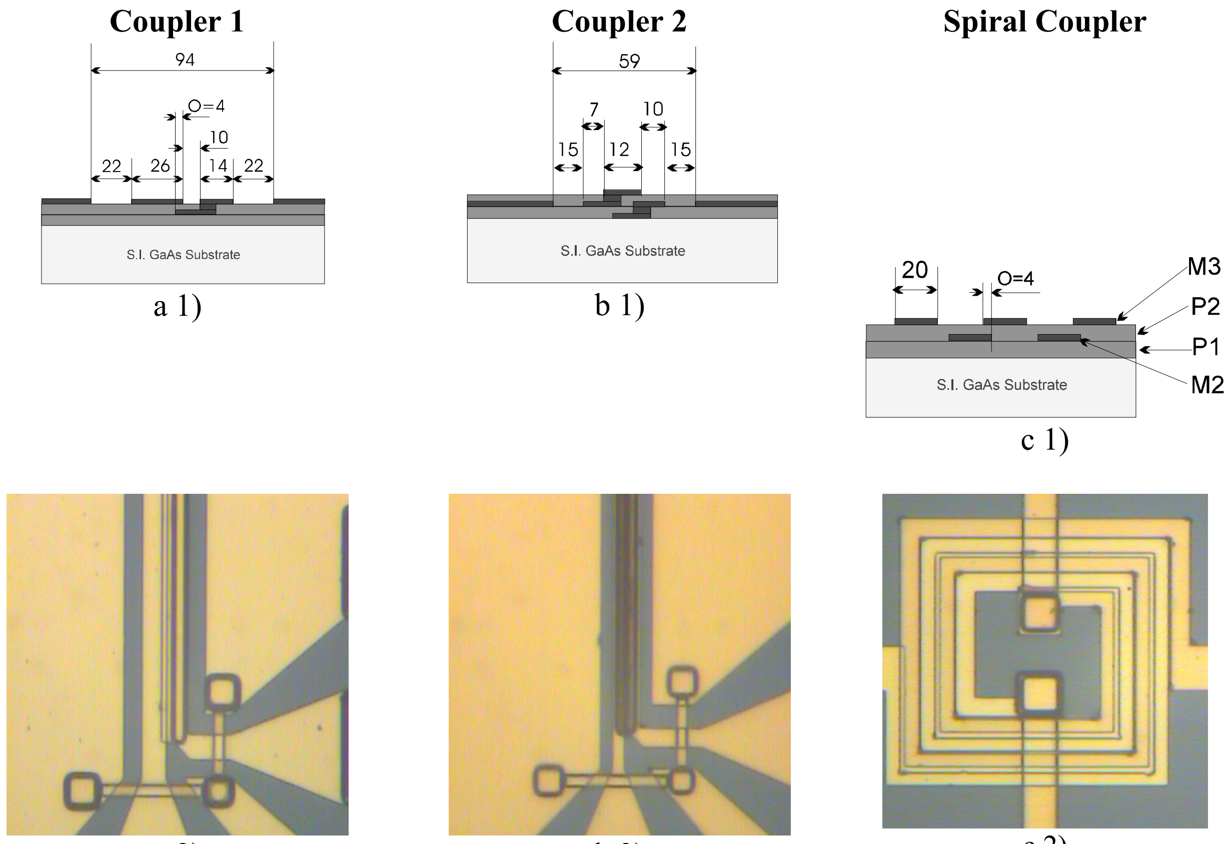

a 1) b 1) c 1)

a 2) b 2) c 2)

The length of directional multilayer couplers is designed to be a quarter wavelength at centre frequency. A lower centre frequency would be required to achieve lower frequency operation but this means longer coupled lines are required. The electrical performance of a coupler is determined by its coupling factor, isolation and directivity. One of the requirements for directional couplers is to maximise the coupler directivity and thus the isolation.

The multilayer couplers in this work have been fabricated using three layers of metals and two layers of sandwich dielectrics. In realising these multilayer structures, several processing aspects have been studied including polyimide spin, curing, etching and metal contact formation. In the fabrication of these structures, different metal layers need to be interconnected properly through the etched windows of the polyimide insulating layers as shown in Fig. 1. The polyimide interconnection windows were formed by oxygen plasma reactive ion etching (RIE) through a protecting photoresist layer patterned using the lithography process. In order to optimise the polyimide etching process, different polyimide etching conditions have been tried including varying plasma power, chamber pressure and gas flow rate.

Cross-sections of three different coupler structures are shown in Figs. 1a1, 1b1 and 1c1. The thickness of Au layer (M1, M2 and M3) was about 0.8 μm. The isolating polyimide layers between metal layers were 2.5 μm thick. All the multilayer directional couplers are fabricated on semi-insulating GaAs substrates at the University of Manchester. The semi-insulating GaAs substrate thickness is 500 μm with $\varepsilon_r = 12.9$.

Results and discussions.

Coupler 1

Fig. 1.a1 shows the cross-sectional view of coupler 1. It can be seen that the top metal

TABLE 1: Momentum simulation of coupler 1 at f = 14GHz

	Overlap size μm			**Polyimide thickness, μm**	
Parameters	2	4	6	1.1	2
Isolation (dB)	27.9	23	20.13	14	25
Coupling (dB)	6.0	5.4	4.84	5.1	5.2
Directivity (dB)	21.9	17.6	15.29	11.1	17.2

(M3) is offset and overlay (overlap) on the lower metal layer (M2), therefore besides the edge coupling mechanism, the structure also incorporates a broadside coupling between different layer of metals. The top layer (M3) is connected through a long polyimide etched window to the lower metal level as shown in Fig. 1.a2. It can be seen that the lower level metal is extended to the underneath of the other branch thus a broadside coupling can be achieved. With this design the insertion loss of conductor can be greatly reduced.

The conductive tracks of the coupler are much wider than those used for interdigitated couplers and are less sensitive to process variations. Between each port and the coupled line section a bridge connection attached the coplanar grounds on both sides of the centre. These underpass connections are necessary to keep the potential equal on separate grounds and thus avoiding the propagation of unwanted modes.

Using ADS Momentum simulation, Table 1 shows the effects of varying the overlap at 14 GHz. By increasing the overlap area, the coupling factor is improved as a result of broadside coupling. Subsequently, this will also reduce the isolation; hence an overlap of 4 μm can be used as a tradeoff. Further increase in the isolation can be achieved by using a thicker polyimide, also shown in Table 1. From the simulation results it is clear that by increasing the polyimide thickness to around 2 μm, an isolation factor of 25 dB can be achieved. Further simulation results showed that increasing this by 3 μm the isolation could be improved to 30 dB.

The length of coupler 1 was designed to be a quarter wavelength at a centre frequency of 16 GHz, giving a length of 2 mm. The widths of the conductors used are 26 μm and 14 μm, which are much wider than the conductors used in interdigitated couplers. The overlap size is 4 μm. A micrograph of the coupler 1 is shown in Fig. 1.a.2.

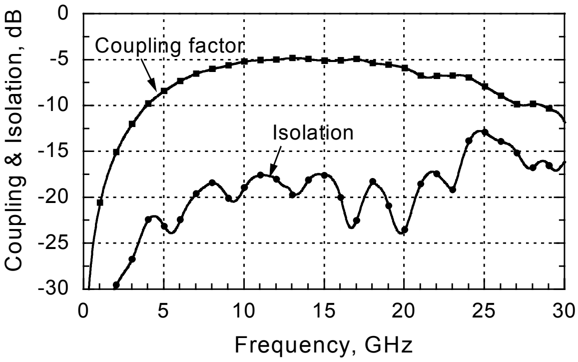

Fig. 2. Measured performance of the coupler 1

The measured performance of the coupler 1 is shown in Fig. 2. The coupling factor of 5 dB is achieved at the centre frequency of 16 GHz. The measured insertion loss is less than 1 dB. Over the frequency range up to 20 GHz the isolation is better than 20 dB. It maintains the isolation of 17 dB over the frequency range up to 40 GHz.

Coupler 2

Fig. 1.b1 shows the cross-sectional view of coupler 2, which is an alternative to design of couple 1. It can be seen that both coupling branches employ two metal layers providing twice more offset broadside coupling than that of the coupler 1, which gives the main mechanism for this coupler. The interconnections are formed through a long polyimide window via. Its double size broadside coupling between the conductors provides better coupling factor. Its width is only about a half that of couple 1, which makes the coupler more compact. However this structure can be slightly more lossy, because the edge coupling is through polyimide instead of being through the air as it is in coupler 1.

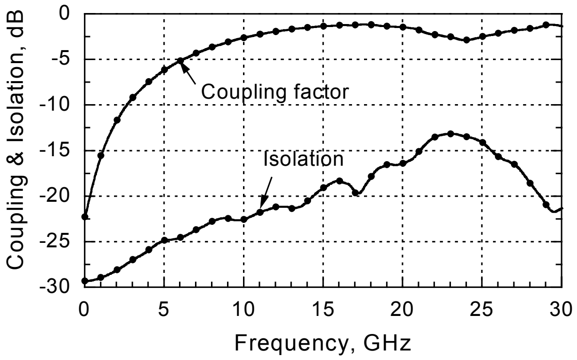

Fig. 3. Measured performance of a coupler 2

The centre frequency of coupler 2 was designed to be 16 GHz, giving its length of 2 mm. The width of the conductors used is 12 μm and the overlap is 2 μm. The gap size for edge coupling is 15 μm.

The measured performance of the coupler 2 is shown in Fig. 3. The coupling factor of 1.6 dB is achieved at the centre frequency 16 GHz. This excellent achievement is due to tight broadside coupling between two branches. The coupler exhibits isolation better than 15 dB over the frequency range up to 30 GHz.

Spiral coupler

Studied of planar spiral transformers have illustrated that they can be effectively modelled as coupled-line elements [4,5]. This leads to the conclusion that a transformer could act as a quadrature coupler if connected as a four-port. The spiral type coupler has the advantages of compact layouts and increased mutual coupling. The centre frequency is very close to that of the unwound length. Fig. 1.c1 shows the cross-sectional view of the spiral coupler. The coupler has two metal spiral (M2 and M3) that are vertically offset by a polyimide layer (P2) as the dielectric layer. In this coupler structure all three types of coupling technique, i.e. edge coupling, offset parallel broadside coupling and mutual coupling can be found. The width of the conductors used is 20 μm and the overlap is 4 μm.

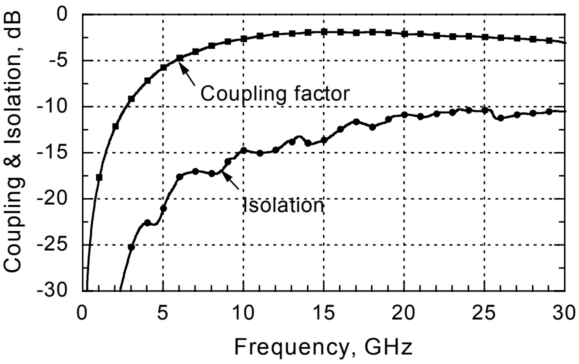

Fig. 4. Measured performance of a spiral coupler

The measured performance of the spiral coupler is shown in Fig. 4. The coupling factor of 1.9 dB is achieved at the frequency 16 GHz. This excellent achievement is due to a combination of edge coupling, offset parallel broadside coupling and mutual coupling. However the coupler exhibits isolation better than 10 dB over the frequency range up to 40 GHz. This relatively small isolation is due to very tight coupling, especially the mutual coupling.

Comparison with an active coupler

An active coupler based on pHEMT devices is used for comparison of the performance of the fabricated multilayer passive couplers detailed above. The active coupler was fabricated in a GaAs foundry.

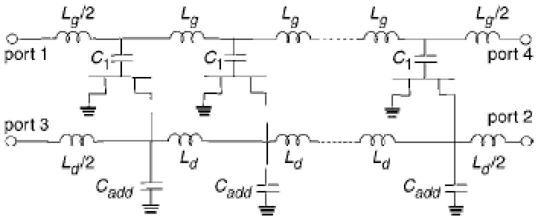

Fig. 5. Lumped element coupler circuit for the pHEMT coupler

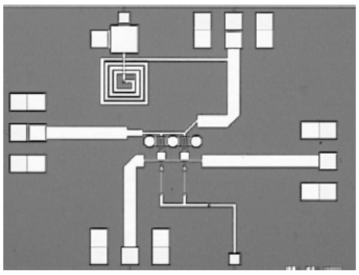

Fig. 6. Micrograph of fabricated planar active coupler based on pHEMTs

Fig. 5 shows lumped element coupler circuit based on distributed amplifier topology for a non-reciprocal coupler [1]. Although this technique has some limitations in the application where a directional coupler would be used, the fact that it is broadband and can be easily implemented in MMIC form attracts RF designers.

It is apparent from the design methodology for the active and passive couplers that a fundamental difference exists between the way the coupling factor is set. The passive coupler requires the setting and control of the transmission line overlap dimension, whereas the active coupler requires a series gate capacitor to be determined for the appropriate coupling factor.

An important factor in the MMIC implementation of couplers is the area of GaAs required to realise the design. The multilayer passive couplers requires a minimum area of 2 mm x 0.2 mm for coupler 1, and 2 mm x 0.15 mm for coupler 2 without meandering the transmission lines which could be employed to reduce the length. While the spiral coupler needs at least 0.4 mm x 0.4 mm area. Implementation of these couplers also requires access to a MMIC process capable of multilayer topology. The active coupler has an intrinsic area of only 0.25 mm x 0.46 mm, although including bias elements means an area of 0.80 mm x 0.46 mm is required which would be regarded as satisfactorily small for most applications where high power and intermodulation is not an issue. Also, a standard MMIC technology process is sufficient to implement this circuit.

The electrical performance of a coupler is determined by its coupling factor, isolation and directivity. Both the passive couplers and active coupler achieve a coupling factor better than 5 dB over the wide range of frequency as shown Fig. 7.a. The best coupling factor of 1.6 dB is provided by coupler 2 at the centre frequency of 16 GHz. The active coupler achieves 5 dB coupling factor over more than three octaves. The passive coupler is also broadband, although its operating band has been designed for higher frequencies up to 30 GHz at the expense of lower frequency performance. A lower design centre frequency would be required to achieve lower frequency operation but this means longer coupled lines are required. On the other hand, there are no size implications in achieving low frequency performance with the active coupler.

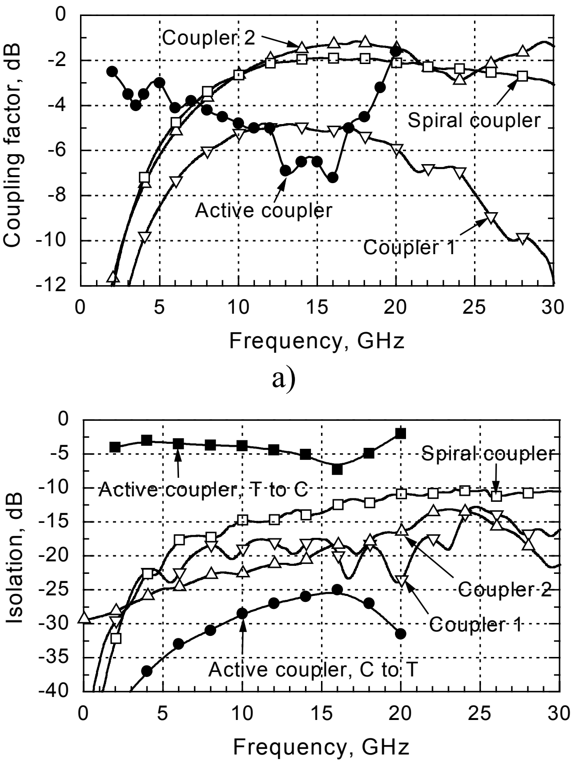

a)

b)

Fig. 7. Comparison of the performance between the three passive couplers and the active coupler

All the multilayer passive couplers exhibit isolation of 10 dB over the frequency range up to 30 GHz, as shown in Fig. 7.b. Coupler 1 provides the best isolation that is better than 20 dB over wide frequency band. The multilayer coupler is reciprocal, hence the transmission port and coupled port are isolated. In contrast, the active coupler is non-reciprocal and the isolation from the coupled port to the transmission port is greater than 26 dB, as shown in Fig. 7.b. but the isolation is poor (5 dB) from the transmission port to the coupled port. Therefore, the active coupler requires additional buffer circuitry on the transmission port to improve the isolation [1].

Conclusion

In this work two GaAs microwave couplers are designed, fabricated and tested. In the design optimization of passive couplers it was shown that by varying the overlap area one could increase the coupling and by selecting the appropriate thickness of polyimide, the isolation can be significantly improved. This provides a flexible design for manufacturing inexpensive microwave couplers.

In comparing the design and implementation of these two components, it was noted that both types of coupler have their relative merits and variations in implementation method.

References

1 Parkinson, G. and Paul, D.K., 2004, IEE Electronics Letters **40**, 810-811.

2 Wen, C P, 1970, IEEE Trans. Microwave Theory Tech., **MTT-18**, 318-322.

3 Gillick, M., Robertson, I.D., and Joshi, 1993, Microw. Opt. Technol. Lett. **6**, 720-723.

4 Engels, M., Jansen, H.R., Daumann, W., Bertenburg, R.M., and Tegude, F.J., 1995, IEEE MTT-S Int. Microwave Symp. Digest 1995, 1635-1638.

5 Wiener, L., Jansen, H.R., Robertson, I.D., IEE Colloquium on Computer aided design of microwave circuits, Digest No **99**, V1-5.

Acknowledgements

The work reported in this paper was funded by the Electro-Magnetic Remote Sensing (EMRS) Defence Technology Centre, established by the UK Ministry of Defence and run by a consortium of SELEX Sensors and Airborne Systems, Thales Defence, Roke Manor Research and Filtronic.